01.1;02.2;13.2

Theoretical dependence of the target threshold sputtering energy on the incidence angle of primary ions

© A.N. Pustovit

Institute of Microelectronics Technology and High Purity Materials, Russian Academy of Sciences, Chernogolovka, Moscow oblast, Russia
E-mail: pustan@iptm.ru

Received March 30, 2022
Revised October 22, 2022
Accepted November 4, 2022

To calculate the angular dependence of the threshold sputtering energy on the ratio of the target masses and incident ions, the target surface blocking phenomenon is used. It is established that the angular dependence of the threshold sputtering energy varies inversely proportional to the cosine of the incidence angle of the primary beam on the target (the angle is measured from the normal to the target surface) to power $s/2$ (s is a power exponent in the interaction potential of colliding particles). A comparison with the literature data is carried out.

Keywords: sputtering, threshold energy, shading cone, angle of ions incidence.

DOI: 10.21883/TPL.2023.01.55343.19206

Ion-beam sputtering is used in low-energy ion irradiation of materials [1] and in plasma physics [2]. The sputtering process is initiated at a certain initial energy of primary ions E, which is called threshold sputtering energy E_{th}. Under normal incidence of the primary beam (atomic number Z_1, mass m_1) onto a target (Z_2, m_2), E_{th} is a specific value characterizing the ion–target system and varies from 10 to 450 eV (see Fig. 4.35 in [3]). Experimental data on the dependence of E_{th}/U_0 (U_0 is the sublimation energy of target atoms) on m_2/m_1 are characterized by a wide scatter (especially in the $m_2/m_1 < 50$ range) that is attributable to differences between the physical properties of systems and difficulties of separation of low-energy ion beams (the results were obtained primarily in discharge plasmas). Large variations are observed for $\sim 20\%$ of targets (the greatest ones correspond to C). At the same time, a functional dependence of E_{th}/U_0 on m_2/m_1 is observed. The authors of [3–5] tried to characterize this dependence using empirical formulae in the $10^{-1}-2\cdot 10^2$ range of mass ratios, but a single unified formula proved elusive. The use of computer simulation methods for calculating sputtering coefficients Y in the region of $< 10^{-4}$ atom/ion is ineffective due to a steep increase in calculation time. This is the reason why E_{th} is considered to be impossible to calculate with the use of molecular dynamics simulation [6]. To date, experimental studies of E_{th} have been performed under normal incidence of an ion beam. Only one study [7], where E_{th} was examined for a carbon target at incidence angles β of 0 and 80° (measured from the normal to the target surface), has been published.

The determination of dependence of E_{th}/U_0 on m_2/m_1 at various angles β is one of the key issues in sputtering and is the aim of the present study.

At E_{th}, atoms escape from the upper layer of an amorphous target material with interatomic distance d [7]. This condition was used to calculate the dependence of E_{th}/U_0 on m_2/m_1 for $\beta = 0°$ in [8], where escape depth h of sputtered particles (measured from the target surface) at E_{th} was assumed to be equal to zero. The obtained formula provides a fine fit to the experimental data throughout the entire m_2/m_1 variation range. The results of further calculations for $\beta \neq 0°$ matched the results for $\beta = 0°$. Note that the formula for Y in [8] yields a zero sputtering coefficient at $h = 0$.

A phenomenon related to target surface blocking at blocking energyE_{bl} [9] was used to solve the supplied problem. This blocking arises due to the extension of a shading-cone vertex, which grows in size to the interatomic distance in the target, at ion energy E_{bl}. Depending on the particle parameters, the value of E_{bl} varies within the $\sim 6-30$ eV range.

The distance of largest approach of particles in the case of a head-on collision (b_s) is the key quantity for characterizing the shading-cone vertex. The value of b_s for paired repulsive power interaction potential $U(r)$ is determined using equality $U(r) = E_0$ [9]:

$$b_s = \left(\frac{Z_1 Z_2 q^2 k_s}{s a E_0}\right)^{1/s} a, \qquad (1)$$

where q is the electron charge, $E_0 = m_2 E/(m_1 + m_2)$ is the relative energy of particles, $k_s = [(s-1)/e]^{s-1}$, s is the power exponent, $a = 0.8853 a_0 (Z_1^{2/3} + Z_2^{2/3})^{-1/2}$ is the screening length, and a_0 is the Bohr radius.

The shading-cone vertex has the shape of a hemisphere with radius b_s at energies $\sim E_{bl}$. At $E \leqslant E_{bl}$, two neighboring hemispheres located at distance d intersect and prevent an ion from penetrating into a target (Fig. 1, *a*). At $E > E_{bl}$, a gap $d - 2b_s$ in size, which allows an ion to penetrate into a target, forms between these hemispheres (Fig. 1, *b*),

Calculated values of distance b_s of largest approach of particles for nickel sputtered by ions with threshold energies $E_{th}(0)$

Ion	Atomic number of ion Z_1	Threshold energy $E_{th}(0)$, eV [11]	Power exponent s	Distance of largest approach b_s, nm
$^{1}H^{+}$	1	66.8	1.31	0.1235
$^{2}D^{+}$	1	34.12	1.492	0.1237
$^{3}T^{+}$	1	24.69	1.592	0.1237
$^{4}He^{+}$	2	20.67	1.88	0.1232
$^{12}C^{+}$	6	17	2.4	0.1236
$^{20}Ne^{+}$	10	19.57	2.58	0.1233
$^{40}Ar^{+}$	18	26.29	2.76	0.1234
$^{84}Kr^{+}$	36	38.42	2.98	0.1235
$^{132}Xe^{+}$	54	48.88	3.12	0.1233

Let us denote the dependence of threshold sputtering energy on ion incidence angle β as $E_{th}(\beta)$. Substituting E for $E_{th}(\beta)$ in formula (1), we then also replacing b_s for $b_s(\beta)$. The initiation condition for sputtering is $E_{th}(0) \gg E_{bl}$ [9]. The values of b_s were calculated using formula (1) for Ni ($Z_2 = 28$, $m_2 = 58.71$, $d = 0.2492$ nm [10]) sputtered by different ions with threshold energies $E_{th}(0)$ [11] to estimate the gap size (see the table). The obtained gap size is $2.5 \cdot 10^{-3}$ nm. The gap grows with energy E.

Partial or complete shading of the gap occurs at ion energy $E_{th}(0)$ and $\beta > 0°$. The gap size in plane $x'z'$ depends on angle β due to the variation of distance d along axis x' (Fig. 1, *c*):

$$d' = d\cos\beta. \qquad (2)$$

The shapes of figures in planes xz and $x'z'$ in the case of ion penetration into a target at $\beta = 0°$ and $\beta > 0°$ are presented in Fig. 2. The area of the gap adjacent to one target atom in Fig. 2, *a* at $E_{th}(0)$ is equal to the area of the ring enclosed between two circles with diameters d and $2b_s(0)$. Note that the ring area in Fig. 2, *a* is 2.3% of the area of the outer circle for Ni (calculated using the data from the table). At $\beta > 0$, the outer circle turns into an ellipse with diameters d and d'. If the ion beam parameters remain unchanged, the areas of inner circles are equal, while the ellipse is smaller in area than the initial outer circle and may overlap with the inner circle. The probability of initiation of sputtering then decreases, and a greater gap area is needed to increase it. This is achieved by raising the threshold sputtering energy and reducing b_s (see (1)). Therefore, condition $E_{th}(\beta) > E_{th}(0)$ should be satisfied. This case is illustrated in Fig. 2, *b*.

One of the definitions of E_{th} is that sputtering coefficient Y at this ion energy is zero [5]. Probabilistic methods are used to analyze the sputtering process [10]. Since the overall area of the outer figure changes with β, the probability of initiation of sputtering at a fixed ion flux density is proportional to the ratio of the ring area to the outer figure

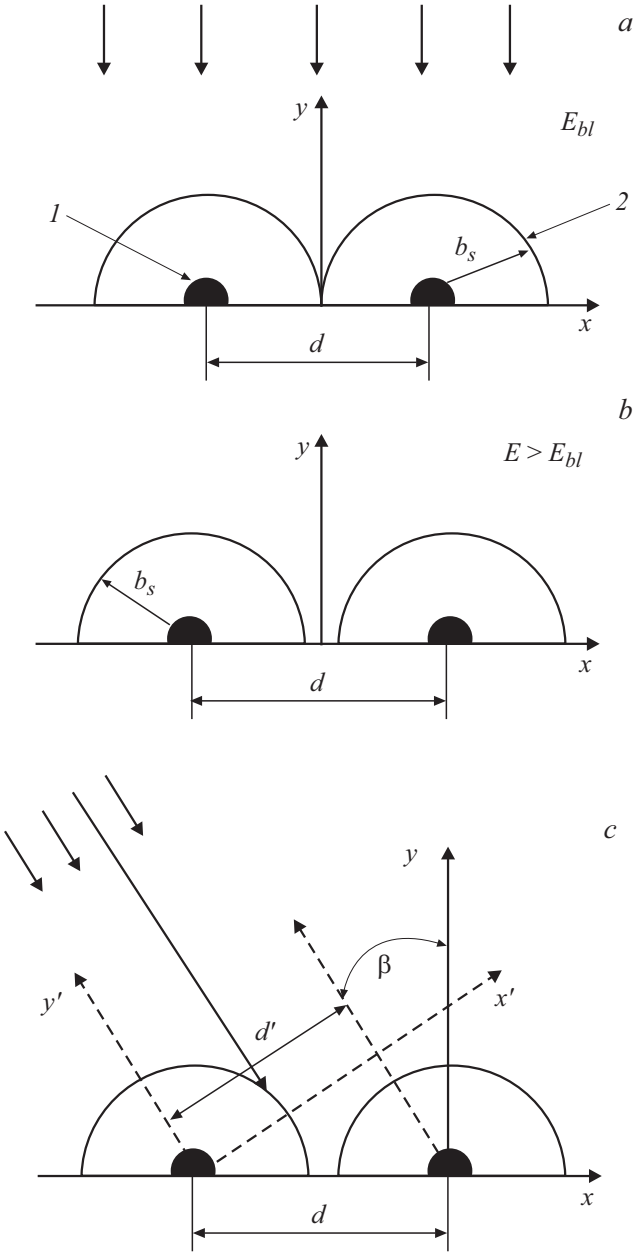

Figure 1. Diagrams of surface blocking and the emergence of a gap between atoms under normal incidence (*a*, *b*) and incidence at angle β (*c*) of the primary ion beam onto a target. *1* — Target atom, *2* — shading-cone vertex. Axes z and z' are directed perpendicularly to the image plane and originate at the center points of the corresponding coordinate systems (xy and $x'y'$).

(circle or ellipse) area:

$$W(\beta) \propto \frac{(d/2)^2\cos\beta - b_s^2(\beta)}{(d/2)^2\cos\beta} = 1 - \frac{4b_s^2(\beta)}{d^2\cos\beta}. \qquad (3)$$

At $Y = 0$, it may be assumed that $W(0) = W(\beta)$. Taking (3) into account, we find

$$\frac{W(\beta)}{W(0)} = 1 = \frac{d^2 - 4b_s^2(\beta)/\cos\beta}{1 - 4b_s^2(0)}. \qquad (4)$$

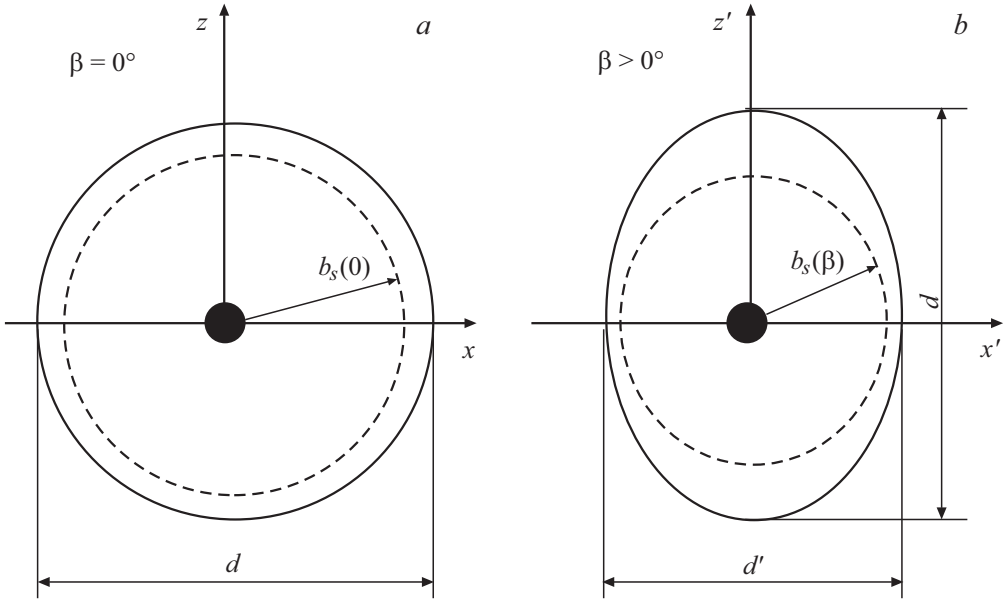

Figure 2. Shapes of figures for potential penetration of ions into a target under normal incidence of an ion beam with energy $E_{th}(0)$ (a) and oblique incidence of an ion beam with energy $E_{th}(\beta)$ (b).

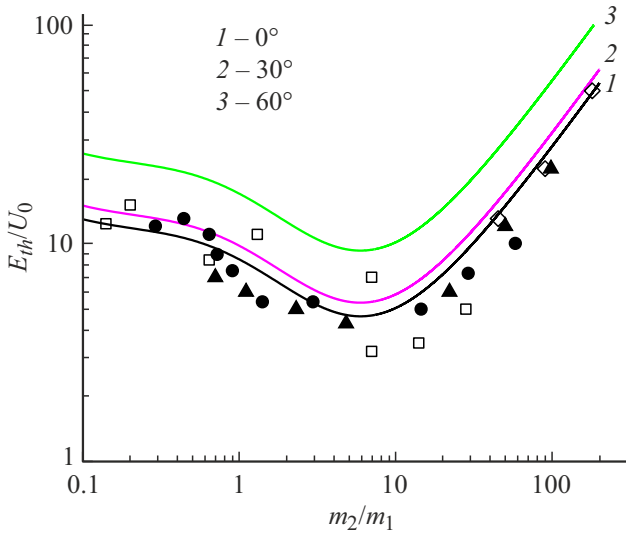

Figure 3. Dependences of E_{th}/U_0 on m_2/m_1 for $s = 2$ and incidence angles $\beta = 0$, 30, and 60° of the primary beam. Experimental results [3]: squares — Si, circles — Ni, triangles — Mo, diamonds — Au.

Inserting the values of $b_s(0)$ and $b_s(\beta)$ from formula (1) into (4), we obtain the final result

$$E_{th}(\beta) = \frac{E_{th}(0)}{\cos^{s/2}\beta}. \qquad (5)$$

Figure 3 presents the dependences of E_{th}/U_0 on m_2/m_1 calculated in accordance with (5) for $s = 2$ and $\beta = 0$, 30, and 60°. The curve for $\beta = 0°$ was plotted using the equation and the data from [8]. Experimental data for Si, Ni, Mo, and Au at $\beta = 0°$ were taken from [3]. Note that all the curves in Fig. 3 were plotted with inelastic losses factored in, since they were taken into account in the calculation of curve *1* [8]. It can be seen from Fig. 3 that the theoretical curves (at least those for angles $\beta \leqslant 30°$ are located close to each other, and a number of experimental points are imposed on them for $\beta = 0°$. Therefore, we should add the following reasons for a wide scatter of experimental data for $\beta = 0°$ to those that were already mentioned in [3]. One of them is related to the target surface roughness on an atomic level. This surface roughness may be of natural origin or be formed in the process of long-term sputtering on the target surface irradiated by ions with an energy of $E_{th}(0)$. The other reason is associated with the probable sputtering of a target by neutral plasma atoms. They may approach the target surface at various angles. The combined influence of these two factors makes it impossible to argue that sputtering proceeded exclusively at $\beta = 0°$.

The present study differs from earlier papers (e.g., [2,5,12,13]) in that the process at $E < E_{th}(\beta)$ (and then at $E = E_{th}(\beta)$) is analyzed. The authors of [2,5,13] used semi-empirical approaches to calculation of the sputtering yield [1], starting their analysis with $E > E_{th}(\beta)$ and proceeding to $E \to E_{th}(\beta)$. In addition, each published work has its own features: (1) the formula based on Silsbee chains in [12] is inapplicable to sputtering by heavy ions, since only one reorientation collision is taken into account [13]; (2) inelastic energy losses in [13] were neglected, only two of the considered nine scenarios yielded the lowest E_{th} with not too shallow β and a large number of collisions [2], and the shading (blocking) effect was taken into account only at large angles β; (3) the results of experiments with D_3^+ in [5] are likely to be erroneous due to the possible molecular effect at low energies [14], the blocking effect

was not mentioned in [2,5], and a large number of collisions were used in calculations.

It was found [7,8] that three inelastic collisions of an ion are needed at energy $E_{th}(0)$ to knock an atom out of the upper layer: (1) collision with a surface atom on entry into a target; (2) reflection from the inner layer toward the surface (rotation by $\sim \pi$); (3) knocking out a surface atom. On the energy scale, $E_{th}(\beta)$ is the boundary between blocking and sputtering regions. Semi-empirical approaches rely on the calculation of Y (i.e., operate at the sputtering–blocking boundary) and do not always make a correct allowance for blocking. This is the reason why calculated $E_{th}(\beta)$ values decrease with increasing angle β. When the shadowing effect is taken into account (at $\beta \geqslant 60^\circ$) [13], $E_{th}(\beta)$ increases. The present study was carried out for the blocking–sputtering boundary and reaches the opposite conclusion: $E_{th}(\beta)$ should increase with angle β in accordance with formula (5). Taking the definition of E_{th} [5] into consideration, one may state that empirical approaches in [2,5,13] probe the near-threshold sputtering energies.

Unfortunately, it is not possible to compare the results of semi-empirical approaches and the results obtained using formula (5) with experimental data, since such data are unavailable. This problem has been topical for quite some time [5]. However, the results reported below are important in the context of a deeper understanding of the physics of sputtering and improvements in the calculation results of characteristics related primarily to variations of the ion incidence angle.

Funding

This study was carried out under the state assignment. № 075-00706-22-00.

Conflict of interest

The author declares that he has no conflict of interest.

References

[1] B. Rauschenbach, *Low-energy ion irradiation of materials. Fundamentals and application*. Springer Ser. in Materials Science (Springer, Cham, 2022), vol. 324. DOI: 10.1007/978-3-030-97277-6

[2] W. Eckstein, R. Preuss, J. Nucl. Mater., **320** (3), 209 (2003). DOI: 10.1016/S0022-3115(03)00192-2

[3] H.H. Andersen, H.L.Bay, in *Sputtering by particle bombardment. I. Physical sputtering of single element solids*, ed. by R. Behrisch. Topics in Applied Physics (Springer-Verlag, Berlin–Heidelberg–N.Y., 1981), vol. 47, p. 145.

[4] M.D. Gabovich, N.V. Pleshivtsev, N.N. Semashko, in *Puchki ionov i atomov dlya upravlyaemogo termoyadernogo sinteza i tekhnologicheskikh tselei* (Energoatomizdat, M., 1986), pp. 71–111 (in Russian).

[5] W. Eckstein, C. Garciá-Rosales, J. Roth, J. László, Nucl. Instrum. Meth. Phys. Res. B, **83** (1-2), 95 (1993). DOI: 10.1016/0168-583X(93)95913-P

[6] C. Yan, Q.I. Zhang, AIP Adv., **2** (3), 032107 (2012). DOI: 10.1063/1.4738951

[7] R. Behrisch, G. Maderlechner, B.M.U. Scherzer, M.T. Robinson, Appl. Phys., **18** (4), 391 (1979). DOI: 10.1007/BF00899693

[8] A.N. Pustovit, J. Surf. Investig., **11** (5), 1069 (2017). DOI: 10.1134/S1027451017050342.

[9] A.N. Pustovit, J. Surface Investig., **15** (Suppl. 1), S204 (2021). DOI: 10.1134/S1027451022010165.

[10] W. Eckstein, *Computer simulation of ion-solid interactions* (Springer-Verlag, Berlin–Heidelberg, 1991). DOI: 10.1007/978-3-642-73513-4.

[11] W. Eckstein, C. Garcia-Rosales, J. Roth, W. Ottenberger, *Sputtering data*, IPP 9/82 (Max-Planck-Institut für Plasmaphysik, Garching, 1993).

[12] D.E. Harrison, Jr., G.D. Magnuson, Phys. Rev., **122** (5), 1421 (1961). DOI: 10.1103/PhysRev.122.1421

[13] Y. Yamamura, J. Bohgdansky, Vacuum, **35** (12), 561 (1985). DOI: 10.1016/0042-207X(85)90316-1

[14] Y. Yao, Z. Hargitai, M. Albert, R.G. Albridge, A.V. Barnes, J.M. Gilligan, B.P. Ferguson, G. Lüpke, V.D. Gordon, N.H. Tolk, Phys. Rev. Lett., **81** (3), 550 (1998). DOI: S0031-9007(98)06668-X